Asp 46 Can Substitute for Asp 96 as the Schiff Base Proton Donor in Bacteriorhodopsin†

Matthew Coleman, Anders Nilsson, Terence S. Russell, Parshuram Rath, Rashmi Pandey, and Kenneth J. Rothschild*

Physics Department and Molecular Biophysics Laboratory, Boston University, Boston, Massachusetts 02215

Received June 30, 1995; Revised Manuscript Received September 18, 1995®

ABSTRACT: Bacteriorhodopsin functions as a light-driven proton pump in the purple membrane of *Halobacterium salinarium.* A variety of studies have established that a proton is transferred over an approximately 10 Å distance from Asp 96 to the retinylidene Schiff base during the M → N transition of the bR photocycle. In order to further explore the mechanism of this Schiff base reprotonation, we compared the properties of the double mutant Thr 46 → Asp/Asp 96 → Asn (T46D/D96N), the single mutants Asp 96 → Asn (D96N) and Thr 46 → Asp (T46D), and wild-type bR. In contrast to D96N, which exhibits a very slow M decay, T46D/D96N has an M decay close to that of wild-type bR. FTIR difference spectroscopy detects bands in the carboxyl and carboxylate stretch region of T46D/D96N consistent with the deprotonation of Asp 46 during the M → N transition. In addition, bands associated with structural changes of Asn 96 in the mutant D96N are absent in T46D/D96N. Resonance Raman spectroscopy provides evidence that both T46D/D96N and T46D have a long-lived N-like species in their photocycles. These data demonstrate that Asp 46 can substitute for Asp 96 as the proton donor group in the reprotonation pathway of the Schiff base during the M → N transition. However, N decay is delayed in comparison to wild-type bR. This may be due to a partial block in the proton pathway leading from the cytoplasmic medium to Asp 46.

Bacteriorhodopsin (bR)[1] functions as a light-driven proton pump in the purple membrane of *Halobacterium salinarium* (*H. salinarium*) (Stoeckenius & Bogomolni, 1982; Rothschild & Sonar, 1995). Upon absorption of a photon by the bR retinylidene chromophore, a photocycle occurs consisting of a series of metastable intermediates with distinct visible absorptions:

$$bR_{570} \rightarrow K_{630} \rightarrow L_{550} \rightarrow M_{412} \rightarrow N_{550} \rightarrow O_{640} \rightarrow bR_{570}$$

Based on progress from several laboratories, a model has emerged which provides a framework for understanding the bR photocycle and proton pump mechanism (Braiman et al., 1988; Butt et al., 1989; Otto et al., 1989; Lanyi, 1992; Rothschild & Sonar, 1995). According to this model, proton translocation can be divided into two distinct phases corresponding to proton release, which occurs during the early phase of the photocycle (~40 μs), and proton uptake, which occurs in the slower late phase of the photocycle (~5 ms). In wild-type bR, proton release involves a proton transfer from the Schiff base to Asp 85 (L → M) (Braiman et al., 1988) and an almost simultaneous ejection of a proton into the outer medium from an as yet unidentified group (Otto et al., 1990). Proton uptake involves the reprotonation of the Schiff base via transfer of a proton from Asp 96 through an as yet undetermined proton pathway (M → N) and the reprotonation of Asp 96 via uptake of a proton from the cytoplasmic medium (N → O). A switch in the Schiff base accessibility from the extracellular to cytoplasmic medium is also expected to occur during the bR photocycle (Kataoka et al., 1994; Tittor et al., 1994). This may correspond to a conformational change involving the rearrangement of membrane embedded α-helical structure which occurs during the M → N transition (Rothschild et al., 1993; Subramaniam et al., 1993) and may involve movement in helix C near Asp 96 (Steinhoff et al., 1994).

In this paper, we have focused on the proton uptake phase of the bR photocycle. An important question is how a proton is transferred from Asp 96 to the Schiff base over a distance of approximately 10 Å (Henderson et al., 1990). One possibility is that there exists a proton wire which is formed by a hydrogen-bonded network of hydrophilic residues (*e.g.*, Tyr, Thr, Ser, Asp) and water molecules. Based on both spectroscopic studies (Braiman et al., 1988; Rothschild et al., 1992, 1993) and the electron diffraction derived structural model of bR (Henderson et al., 1990), we have previously suggested that specific residues which might participate in such a transient network include Thr 46, Thr 89, Tyr 185, and Asp 212 (Rothschild et al., 1992, 1993). Alternatively, proton transfer could occur through a transient channel which is opened during the photocycle. Recent dynamic modeling of the bR structure shows how such a pore might be formed (Zhou et al., 1993).

In order to further investigate the Schiff base reprotonation mechanism, we have combined site-directed mutagenesis with a variety of spectroscopic methods. Since Thr 46 is postulated to be a part of the Schiff base reprotonation

† This work was supported by grants from the NSF (MCB 9106017) and the Army Research Office (ARO) (DAAL03-92-G-0172) to K.J.R. A.N. is supported by a postdoctoral fellowship from the Wenner-Gren Center Foundation (Sweden). M.C. is supported by an NIH Training Grant (GM08291-06).

* Address all correspondence to this author, at 590 Commonwealth Ave., Department of Physics, Boston University, Boston, MA 02215.

® Abstract published in *Advance ACS Abstracts,* November 15, 1995.

[1] Abbreviations: FTIR, Fourier transform infrared; PM, purple membrane; bR, bacteriorhodopsin; PCR, polymerase chain reaction; dNTP, deoxynucleotide triphosphate.

0006-2960/95/0434-15599$09.00/0

Scheme 1

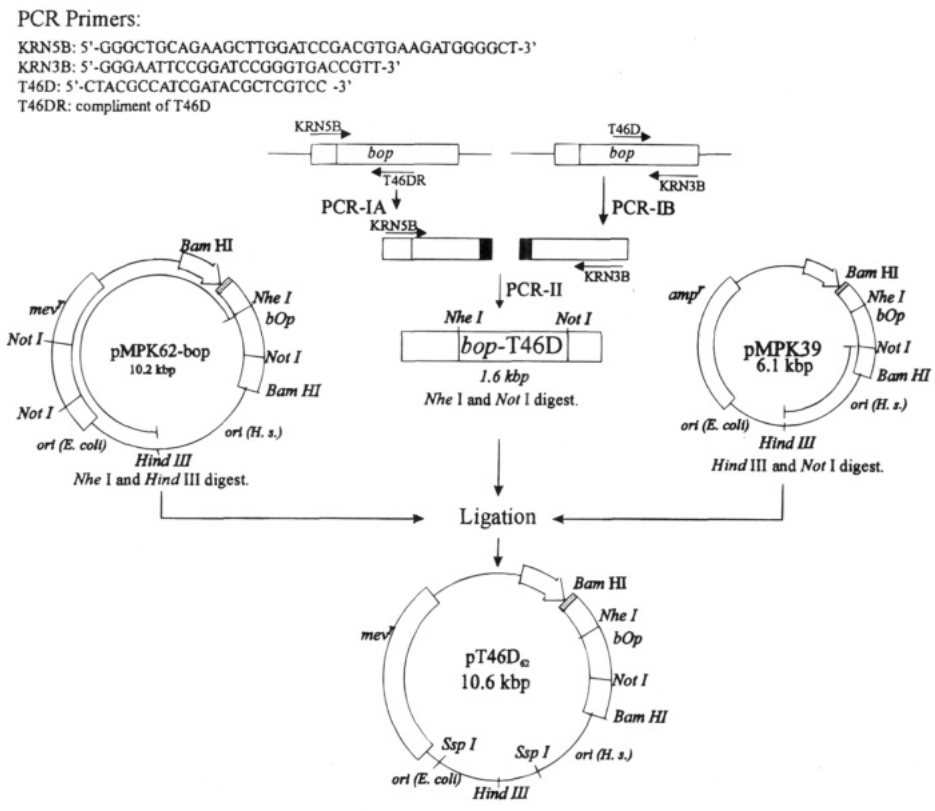

pathway and is proximal to Asp 96 (Marti et al., 1991; Rothschild et al., 1992), a simple prediction is that the double mutant Thr 46 → Asp/Asp 96 → Asn (T46D/D96N) should exhibit a relatively normal M decay. In this case, Asp 46 would be in a position to function as a new proton donor for the Schiff base. In contrast, the single mutation Asp 96 → Asn exhibits a slowed M decay due to the removal of Asp 96 as the internal proton donor for the Schiff base (Butt et al., 1989; Otto et al., 1989). Both FTIR difference spectroscopy and time-resolved visible absorption spectroscopy confirm this prediction and, along with resonance Raman spectroscopy, reveal the existence of a slowly decaying N intermediate in T46D/D96N. We also find that structural changes in Asn 96 that occur in the photocycle of D96N are absent in the photocycle of T46D/D96N. The implications of these results for understanding the Schiff base reprotonation pathway are discussed.

MATERIALS AND METHODS

Materials. All chemical reagents were purchased from Sigma Chemical Co. (St. Louis, MO). Restriction endonucleases and nucleic acid-modifying enzymes were purchased from Promega Corp. (Madison, WI), New England BioLabs (Beverly, MA), and Stratagene Cloning Systems (La Jolla, CA). Plasmid constructs were verified by dideoxy chain termination sequencing using a Sequenase-2 kit (U.S. Biochemical Corp., Cleveland, OH) and [^{35}S]dATP (Amersham, Arlington Heights, IL). Oligonucleotides were synthesized on a 392 DNA Synthesizer (Applied Biosystems Inc., Foster City, CA). The procedures for restriction digestion, DNA purification, DNA ligation, agarose gel electrophoresis, *Escherichia coli* (*E. coli*) DH5α cell transformations, nucleic acid quantitation and purification, and SDS−PAGE electrophoresis have been described earlier (Sambrook et al., 1989).

Plasmid Construction, Protein Expression, and Purification. Polymerase chain reaction (PCR) based mutagenesis (Ho et al., 1989) was used to construct the substitutions Thr 46 → Asp, Asp 96 → Asn, and Thr 46 → Asp/Asp 96 → Asn in the native bacterioopsin *(bop)* gene. Scheme 1 shows the steps for PCR and plasmid construction of T46D. The initial round of PCR mutagenesis (PCR-IA and PCR-IB) generated two fragments of DNA with overlapping sequences (represented by shaded areas) that contain the mutation of interest. In the second round of PCR (PCR-II) the full-length *bop* gene was synthesized with the single mutation. The PCR fragment was then digested and ligated to the two fragments obtained from the pMPK vectors (Krebs et al., 1991, 1993). After the plasmids for the single mutants T46D ($pT46D_{62}$) and D96N ($pD96N_{62}$) were prepared, the $pT46D_{62}$ plasmid was used as the template to make the T46D/D96N double mutant. The primers used for D96N were 5′-TTGTTGTTAAACCTCGCGTTG-3′ and its complement. Typical PCR reactions utilized 10 μM of each primer, 10 ng of pMPK39 (Krebs et al., 1991) or ∼1 μg of *H. salinarium* genomic DNA as a template, 250 μM dNTPs, 0.5 unit of Vent DNA polymerase (New England Biolabs, Beverly, MA), PCR buffer (10 mM KCl, 10 mM $(NH_4)_2SO_4$, 20 mM Tris-HCl (pH 8.8)), 2 mM $MgSO_4$, and 0.1% Triton X-100, in a total volume of 100 μL. The PCR reaction mixture was denatured at 98 °C for 5.0 min and amplified using the following parameters on a Mini-Thermal Cycler (MJ Research, Watertown, MA): 1.5 min at 98 °C; 1.5 min at 37 °C; 1.0 min at 72 °C, for 4 cycles, followed by 11 cycles of 1.5 min at 98 °C; 1.5 min at 55 °C; 1.5 min at 72 °C; and finally 5.0 min at 72 °C. The 1.6 kb PCR generated fragment was restricted with *Not*I and *Nhe*I and ligated to a *Hin*dIII−*Nhe*I fragment from pMPK39 and a *Not*I−*Hin*dIII fragment from pMPK62 (Krebs et al., 1991,

1993). The resulting plasmid was amplified in *E. coli* DH5α cells, purified, sequenced, and then transformed into the strain MPK40 of *H. salinarium* containing a deletion in the *bop* gene (Krebs et al., 1993). Wild-type and mutant strains were grown and purple membrane was isolated using previously described procedures (Oesterhelt & Stoeckenius, 1974).

Static Absorption Spectra. Static absorption spectra of light- and dark-adapted mutants were obtained in solution (25 mM NaP_i, pH 7.0) at 23 °C using a UV/vis spectrometer (Model UV-2101, Shimadzu, Kyoto, Japan). Samples were dark-adapted overnight and then light-adapted as previously described (Duñach et al., 1990b; Sonar et al., 1993).

Time-Resolved Absorption Spectroscopy. Time-resolved difference spectra were measured on samples suspended in 25 mM NaP_i buffer at pH 7.0. As described previously (Duñach et al., 1990a; Sonar et al., 1993), the apparatus consisted of a gated optical multichannel analyzer (Model 1420 UV-enhanced Model 1460 controller; Princeton Applied Research, Princeton, NJ) and a 532 nm pulsed excitation from a frequency doubled Nd-YAG laser (GCR-11, Spectra Physics, Mountain View, CA). The data acquisition window was 100 μs. The delay times given in Figure 2 refer to the time between the laser flash and the initiation time of the data acquisition window. The laser was operated at an output power of 70 mJ/pulse with a pulse width of 7 ns. The repetition frequency of the laser ranged from 0.5 Hz for D96N to 20 Hz for wild-type. The decay kinetics were determined using Peakfit (Jandel Scientific, San Rafael, CA). The data were fit to both double and single exponential functions, for which the number of time points ranged from 7 to 14.

Resonance Raman Spectroscopy. Resonance Raman spectroscopy of wild-type bR and T46D/D96N was performed using an apparatus previously described (Rath et al., 1993a,b). A 250 μL wild-type or mutant purple membrane sample (25 mM NaP_i buffer at pH 8.0 with an absorbance of 1 OD at 570 nm) was placed in a quartz spinning cell of 19 mm internal diameter and rotated with a time period of 22 ms. Under these conditions, the sample is exposed by the probe laser beam to periodic pulses of 1.8 μs duration every 22 ms. This prevented contributions to the spectrum from intermediates with lifetimes shorter than 22 ms. Samples were excited by a cylindrically focused 514.5 nm CW laser beam from an argon ion laser (Model I70-4, Coherent Inc., Palo Alto, CA). The scattered radiation was collected at a right angle to the incident laser beam. In order to achieve a low photoalteration rate, the laser power was kept below 8 mW (Mathies et al., 1977; Rath et al., 1993b).

FTIR Difference Spectroscopy. Difference spectra were recorded using methods previously reported (Rothschild et al., 1984; Roepe et al., 1987; Braiman et al., 1988). Samples were prepared by air-drying approximately 100−200 μg/cm^2 of sample on an AgCl window and then rehydrating prior to insertion into a sealed transmittance cell which was mounted in a Helitran cryostat (Air Products, Allentown, PA). The water content of the sample was checked by monitoring the 3400 cm^{-1} peak. All samples were light-adapted at room temperature prior to cooling by illuminating the sample for at least 15 min with a 150 W tungsten light source (Dolan-Jenner Industries, Inc., Lawrence, MA) equipped with a 505 nm long-pass filter. Spectra were recorded at 2 cm^{-1} resolution using either a Nicolet Analytical Instruments 740 or 60SX spectrometer (Madison, WI).

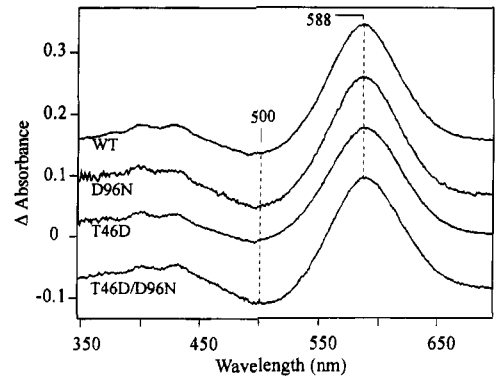

FIGURE 1: Dark → light difference spectra of wild-type bR, D96N, T46D, and T46D/D96N. Difference spectra were obtained by subtracting the absorption spectrum of a dark-adapted sample from the corresponding light-adapted sample. The absorbance scale shown is for the T46D sample. Other spectra were scaled by the following factors: WT, 2.5; D96N, 4; T46D/D96N, 2.5. All samples were measured at 23 °C in pH 7.0, 25 mM NaP_i buffer and at a concentration of 5 μM (see Materials and Methods).

Table 1: M Decay Rate Constants[a]

	Single Exponential Fit			
				τ (ms)
WT				3.2
D96N				243.9
T46D				0.7
T46D/D96N				2.0
	Double Exponential Fits			
	A_1	τ_1 (ms)	A_2	τ_2 (ms)
WT	0.14	7.3	0.86	2.7
D96N	0.43	98.1	0.57	400.2

[a] An integrated area of ±10 nm about the absorption maximum (410 nm) of each time-resolved spectrum (Figure 2) was calculated, and the resulting data were fit to both single and double exponential functions. Note that the double exponential fit of T46D and T46D/D96N gave essentially the same result as the single exponential fit and is not listed. All amplitudes listed are normalized to 1.

RESULTS

Light−Dark Adaptation. As seen in Figure 1, the dark → light difference spectra of all three bR mutants (D96N, T46D, and T46D/D96N) are very similar to that of wild-type bR. In particular, bands are found near 500 nm (negative) and 588 nm (positive) which reflect the normal shift of the bR λ_{max} from 558 to 568 nm upon light adaptation. This result along with time-resolved visible absorption and resonance Raman spectroscopy (see below) demonstrate that while the photocycle kinetics of these mutants are altered, the chromophore configurations of the light- and dark-adapted forms are very similar to those of native bR.

Time-Resolved Visible Absorption Spectroscopy. Figure 2 shows the time-resolved absorption spectra for the late photocycle of wild-type bR and the three mutants. Compared to the M decay time constant of wild-type bR (3.2 ms, for the single exponential fit; single and double exponential fit values are listed in Table 1), the M decay time constant in D96N is significantly slower (244 ms) because of the absence of the Asp 96 Schiff base proton donor (Butt et al., 1989; Otto et al., 1989; Stern et al., 1989). In contrast, the

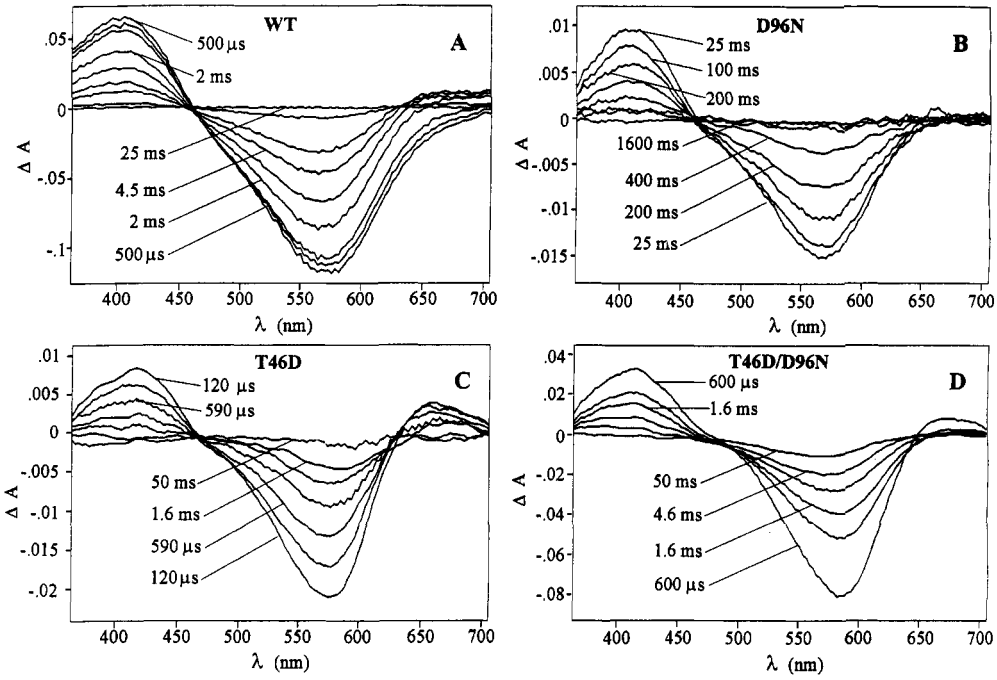

FIGURE 2: Time-resolved visible difference spectra of wild-type bR, D96N, T46D, and T46D/D96N. Time-resolved difference spectra were measured on samples suspended in 25 mM NaP_i buffer at pH 7.0. Difference spectra shown consisted of the average of 300−400 differences of visible absorption spectra measured before and after a specific delay time. Delay times used corresponding to the traces shown in each of the panels were as follows: (A) WT; 0.5, 0.75, 1, 2, 3, 4.5, 6, 12, and 25 ms. (B) D96N; 25, 50, 100, 200, 400, 800, and 1600 ms. (C) T46D; 0.12, 0.35, 0.59, 1, 1.6, and 50 ms. (D) T46D/D96N; 0.6, 1, 1.6, 2.7, 4.6, and 50 ms.

additional substitution of Thr 46 → Asp in the double mutant T46D/D96N produces an M decay slightly faster (2.0 ms) than that of wild-type bR. In agreement with earlier studies, we also find that the single mutant T46D exhibits a faster than normal M decay (0.7 ms)[2] (Rothschild et al., 1993). Figure 2 also shows that although M decay is normal in T46D/D96N, the overall photocycle is slower. For example, a negative band near 570 nm is still observed in the 50 ms trace in T46D/D96N after the intensity of the band at 412 nm has decayed to the base line. A similar, although less dramatic, effect is also observed in T46D in agreement with an earlier study made on T46D expressed in *E. coli* (Rothschild et al., 1993). This effect can be attributed to a partial block in the decay of an N-like intermediate (see below).

FTIR Difference Spectroscopy. Figure 3 compares the FTIR difference spectra recorded for wild-type bR, D96N, T46D, and T46D/D96N at 270 K. Except for the case of D96N,[3] these spectra are all similar to the bR → N difference spectrum recorded by static transmission (Ormos, 1991; Pfefferle et al., 1991), static ATR (Ludlam et al., 1995), and time-resolved FTIR spectroscopy (Bousché et al., 1991, 1992; Braiman et al., 1991; Hessling et al., 1993). In wild-type bR, bands characteristic of the N intermediate are found at 1755 cm^{-1} (+)[4] (Asp 85 carboxyl C=O stretch), 1742 cm^{-1} (−) (Asp 96 carboxyl C=O stretch), 1669 cm^{-1} (−) (α-helix amide I), 1390−1405 cm^{-1} (+) (carboxylate C=O stretch (Bousché et al., 1991) and C_{11}−H in-plane bending (Maeda et al., 1992)), and 1186 cm^{-1} (+) (C−C stretch of

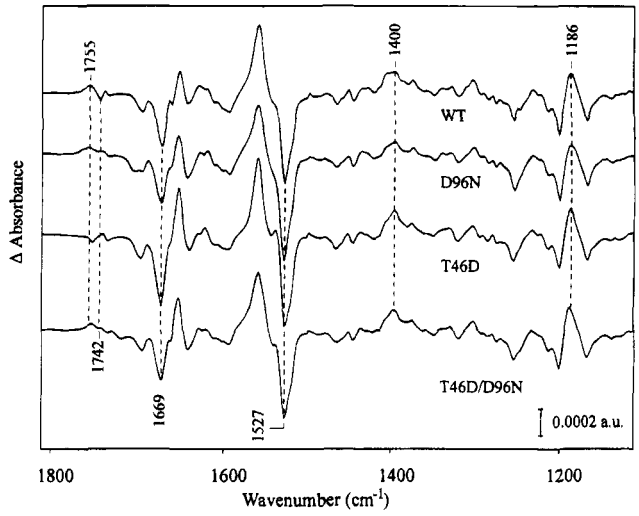

FIGURE 3: FTIR difference spectra for the bR → N transition of wild-type bR, D96N, T46D, and T46D/D96N. All samples were measured at 270 K under identical conditions using FTIR transmission spectroscopy. Spectra shown were recorded at 2 cm^{-1} resolution (see Materials and Methods for additional details).

retinal (Fodor et al., 1988)). A reduction also occurs in the intensity of the negative 1527 cm^{-1} band (ethylenic C=C stretch) relative to the bR → M difference spectrum (data not shown) (Bousché et al., 1991). The latter effect is due to cancellation of the negative C=C ethylenic stretch of light-adapted bR (bR_{570}) at 1527 cm^{-1} by the positive C=C ethylenic stretch mode of N near 1530 cm^{-1} (Fodor et al., 1988).

Despite the overall similarity of these spectra, a more detailed comparison in the carboxylic acid C=O stretch region from 1675 to 1785 cm^{-1} (Figure 4) reveals several key changes which reflect the effects of different substitutions at positions 46 and 96. As expected, the negative band at

[2] An increased M decay rate is also observed in the mutant T46V (Marti et al., 1991; Brown et al., 1993).

[3] In the case of D96N, the difference reflects a mixture of bR → M and bR → N due to the slow M decay of this mutant (Nilsson et al., 1995, unpublished results). See also Sasaki et al. (1992).

[4] (+/−) refer to (positive/negative) bands.

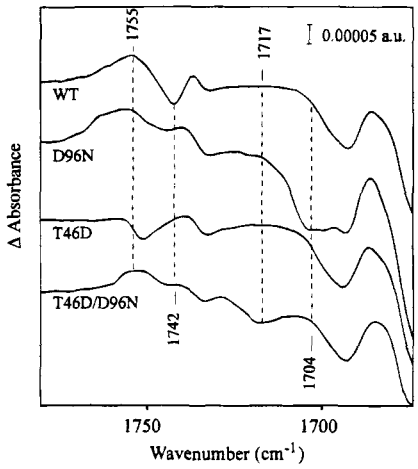

FIGURE 4: FTIR difference spectra for the bR → N transition of wild-type bR, D96N, T46D, and T46D/D96N. Expansion of spectra shown in Figure 3 in the carboxylic acid C=O stretch region from 1675−1785 cm^{-1}.

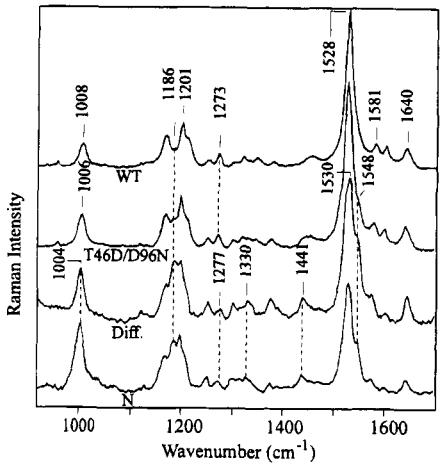

FIGURE 5: Resonance Raman spectroscopy of wild-type bR (WT) and the mutant T46D/D96N. Resonance Raman spectra were measured at room temperature at pH 8.0 in 25 mM NaP_i buffer using a spinning cell apparatus (see Materials and Methods). The difference spectrum (Diff.) was obtained by subtracting the wild-type spectrum from that of T46D/D96N. Subtraction was performed interactively using the program GRAMS/386 (Galactic Industries Corp., Salem, NH) (Sonar et al., 1994b). The spectrum of the N intermediate of wild-type bR was obtained at pH 9.0 (3 M KCl) as previously described (Subramaniam et al., 1991).

1742 cm^{-1} assigned to the deprotonation of the carboxylic acid group of Asp 96 during the M → N transition is completely absent in D96N (Braiman et al., 1988) as well as in the double mutant T46D/D96N. However, in the latter case, a new negative band appears at 1717 cm^{-1} which downshifts to 1710 cm^{-1} due to H/D exchange (data not shown). A simple explanation for this band is that Asp 46 undergoes a deprotonation during the M → N transition similar to the normal deprotonation of Asp 96 in wild-type bR. It is unlikely that the band at 1717 cm^{-1} is due to the Asn 96, since as noted above, it is sensitive to H/D exchange in contrast to Asn 96 in the mutant D96N (Gerwert et al., 1989). Interestingly, a negative band which appears at 1704 cm^{-1} in D96N (Figure 4), assigned to structural changes in Asn 96 during the photocycle (Braiman et al., 1988; Gerwert et al., 1989; Maeda et al., 1992), is absent in the mutant T46D/D96N.

The possibility that Asp 46 deprotonates during the M → N transition in T46D/D96N is also supported by changes observed in the region near 1400 cm^{-1} (Figure 3). In wild-type bR, a positive band appears near 1400 cm^{-1} due to the carboxylate C=O stretch of deprotonated Asp 96 (Bousché et al., 1991). While this band is weak in D96N, an increase in intensity in the same region appears in T46D/D96N, indicating that a different carboxylate group, *i.e.*, Asp 46, is now formed during the M → N transition. However, the analysis of this region is complicated by the presence of an additional band near 1400 cm^{-1} due to the C_{11}−H in-plane bending vibration of the chromophore (Maeda et al., 1992) as well as different amounts of the N intermediate produced in each mutant.

Compared to wild-type, D96N, and T46D/D96N, the spectral changes in the carboxylic acid C=O stretch region of T46D are quite different. Most apparent is the drop in intensity of the band at 1755 cm^{-1} which is assigned to Asp 85. This result is very similar to an earlier study on T46D expressed in *E. coli* (Rothschild et al., 1993), where it was concluded that these spectral changes are due to an upshift of the C=O stretch mode of Asp 96 from 1742 cm^{-1} (−) to near 1755 cm^{-1} (−) caused by a change in its local environment. This would be consistent with an interaction between Asp 96 and Asp 46 in this mutant. The alternative possibility that these changes reflect a deprotonation of Asp 46 and not Asp 96 cannot be excluded (see Rothschild et al. (1993) for additional details).

Resonance Raman Spectroscopy. Spinning cell resonance Raman spectroscopy (Argade & Rothschild, 1982) can be used to probe for the existence of long-lived photointermediates in the bR photocycle (Subramaniam et al., 1991; Rath et al., 1993a; Rothschild et al., 1993; Sonar et al., 1994b) (Figure 5). In addition to bR_{570}, only intermediates with a lifetime longer than the rotational period of the cell (22 ms) should contribute to the resonance Raman spectrum. In the case of T46D/D96N, the accumulation of an N-like 13-*cis* species is indicated by the increased intensity of the 1186 cm^{-1} band. This is characteristic of the chromophore C−C stretch mode of the N intermediate of wild-type bR (Fodor et al., 1988; Nakagawa et al., 1991). The presence of a long-lived N-like intermediate was confirmed by interactively subtracting the wild-type spectrum from the T46D/D96N spectrum. The resulting difference spectrum (Figure 5) is similar to that of the wild-type N intermediate recorded at high pH conditions (Figure 5, bottom trace) (Subramaniam et al., 1991). For example, the double ethylenic bands at 1530 and 1548 cm^{-1} and the bands appearing at 1441, 1330, 1186, and 1004 cm^{-1} nearly approximate the resonance Raman spectrum of the N intermediate in wild-type bR (Fodor et al., 1988; Nakagawa et al., 1991). Also, a strong band at 800 cm^{-1} characteristic of the 13-*cis*/C=N syn configuration of retinal in dark-adapted bR was not found (data not shown). We conclude that, in contrast to wild-type bR, where no N species was detected at pH 8.0, the N intermediate accumulates in T46D/D96N because of a decay which is slower than the 22 ms rotational period of the cell. A similar effect was also previously observed in the single mutants T46D and T46V (Marti et al., 1991; Brown et al., 1993; Rothschild et al., 1993).

DISCUSSION

In this work we have examined the late photocycle properties of several bR mutants with substitutions at Asp

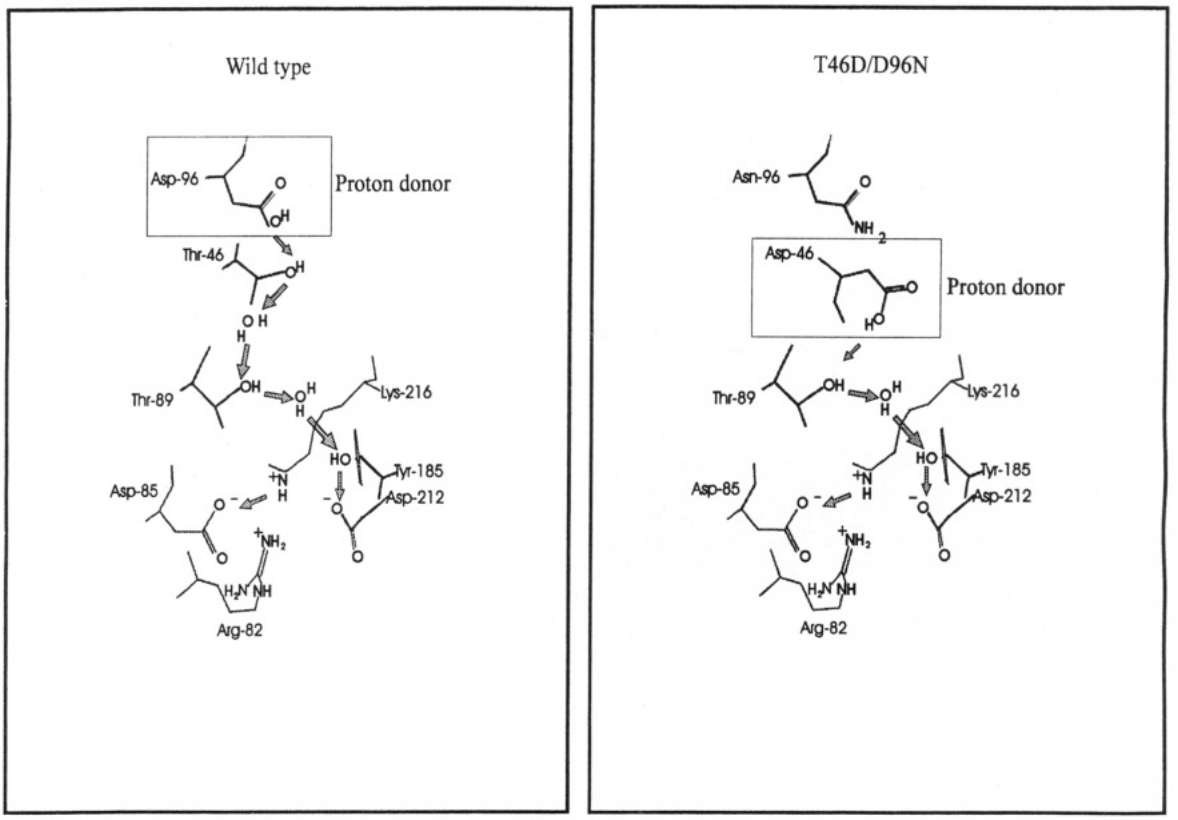

FIGURE 6: Schematic model of possible Schiff base reprotonation mechanism in wild-type bacteriorhodopsin and the double mutant T46D/D96N based on a proton wire. Diagram was adapted from Rothschild et al. (1992) and is based on the structural coordinates for bacteriorhodopsin determined by cryoelectron microscopy (Henderson et al., 1990). Left panel: Suggested proton pathway in wild-type bR where Asp 96 serves as proton donor. Right panel: Suggested proton pathway in T46D/D96N where Asp 46 serves as the proton donor. The path of proton movement is indicated by the shaded arrows. Note that the role of amino acid residues Thr 89, Tyr 185, and Asp 212 in a proton pathway has not yet been established, although site-directed mutagenesis combined with FTIR difference spectroscopy reveals changes consistent with this model (see references (Rothschild, 1992; Rothschild et al., 1992, 1993) for additional details).

96 and Thr 46.[5] Previously, the substitution of Asp 96 with a variety of residues including Asn, Ala, Gly, and Thr has been found to significantly slow the M decay step of the photocycle (Braiman et al., 1988; Mogi et al., 1988; Butt et al., 1989; Drachev et al., 1989; Otto et al., 1989; Stern et al., 1989; Tittor et al., 1989; Thorgeirsson et al., 1991; Danshina et al., 1992; Cao et al., 1993). These results, along with the detection by FTIR difference spectroscopy of Asp 96 deprotonation during the M → N transition (Bousché et al., 1991, 1992; Braiman et al., 1991; Ormos, 1991; Pfefferle et al., 1991; Hessling et al., 1993; Ludlam et al., 1995), established the role of this residue as the Schiff base proton donor. Azide has also been shown to substitute for Asp 96 as the proton donor (Cao et al., 1991; Otto et al., 1989; Tittor et al., 1989). However, little is known about the mechanism during the M → N step of the photocycle which causes Asp 96 to deprotonate and allows a proton to move to the Schiff base. A related question is understanding the movement in the membrane embedded α-helical structure occurring during the M → N transition (Bousché et al., 1991, 1992; Braiman et al., 1991; Pfefferle et al., 1991; Hessling et al., 1993; Rothschild et al., 1993).[6]

One method of exploring these questions is to determine if an Asp residue placed at other positions in the bR sequence could replace Asp 96 in the Schiff base reprotonation mechanism and whether it affects related events in the photocycle. Thr 46 was chosen as a likely candidate for such a substitution because of its close proximity to Asp 96 in the electron diffraction determined structure of bR (Henderson et al., 1990). As shown in Figure 6, this residue, along with several water molecules and Thr 89, Tyr 185, and Asp 212, is in a good position to form part of a proton conducting wire (Rothschild et al., 1992, 1993). In addition, several studies indicate that Thr 46 can interact either directly or indirectly with Asp 96 (Marti et al., 1991; Rothschild et al., 1992; Brown et al., 1994).

In the experiments described here, we found that the strong delay in Schiff base reprotonation caused by the Asp 96 → Asn mutation (D96N) is completely removed by the addition of the second substitution, Thr 46 → Asp (T46D/D96N). In contrast, the double mutant T46V/D96N shows an even slower decay rate than D96N (Brown et al., 1993). In addition, unlike D96N, we detect the deprotonation of an Asp residue in T46D/D96N similar to wild-type bR. *These results demonstrate that Asp 46 can substitute for Asp 96 as an effective Schiff base proton donor in the photocycle of bacteriorhodopsin.* In contrast, it is difficult to determine from earlier experiments (Rothschild et al., 1993) and from the current results which one (or both) of the Asp residues (Asp 96 and Asp 46) serves as the proton donor in the mutant

[5] In related work, we have examined the early photocycle of these mutants (A. Nilsson, T. Russell, M. Coleman, and K. J. Rothschild, unpublished results).

[6] This conformational change may actually occur during the transition between M_I and M_{II} substates of the M intermediate (Varo & Lanyi, 1991), although this has not yet been confirmed.

T46D. In particular, the drop in intensity of the band at 1755 cm^{-1} has been interepreted previously as due to an upshift in the frequency of the negative band at 1742 cm^{-1} assigned to Asp 96 (Rothschild et al., 1993). An alternative explanation, however, might be that this band originates from the deprotonation of Asp 46. One method of distinguishing between these two possibilities would be selective isotope labeling of Asp 96 or Asp 46 using site-directed isotope labeling (Sonar et al., 1994a).

Our results also show that the N decay is slower when Asp 46 serves as the proton donor. In wild-type bR, this step involves reprotonation of Asp 96 due to the uptake of a proton from the cytoplasmic medium (Bousché et al., 1992). Thus, the slower rate in T46D/D96N may be due to an altered pathway for the reprotonation of this residue. This could occur, for example, if the proton pathway leading from the cytoplasm to Asp 46 includes Asn 96, which is expected to act as a barrier for proton transfer when it is part of a proton wire. This is supported by the slower decay of the N intermediate in T46D/D96N compared to T46D (Figure 2C,D). An alternative explanation, however, is that a drop in the effective pK_a of Asp 46 relative to Asp 96 in wild-type bR and Asp 46 in T46D might account for the slower N decay (Rothschild et al., 1993). Several other mutants in this region of the protein including T46V also exhibit slowed N decay (Brown et al., 1993).

The substitution of Asp 96 with Asp 46 as the Schiff base proton donor also does not appear to inhibit the conformational change occurring during the M → N transition, which involves membrane embedded α-helices, as indicated by the presence of the bands at 1669 and 1555 cm^{-1} (Figure 3). While this demonstrates that the deprotonation of Asp 96 is not critical for this structural rearrangement of the protein, it still leaves open the interesting possibility that a key event in the triggering of this conformational change is the production of a negative charge in the vicinity of Asp 96. In this regard, it would be expected that reprotonation of Asp 46 should be correlated with the reversal of this conformational change as is observed for the case of Asp 96 in wild-type bR (Hessling et al., 1993) and the mutant Y185F at high pH (Bousché et al., 1992).

An additional effect of the double substitution T46D/D96N compared to the single substitution D96N is the disappearance of a negative band at 1704 cm^{-1} which has previously been assigned to the C=O stretch of Asn 96 (Gerwert et al., 1989). In D96N, a perturbation of Asn 96 can be understood as a result of changes which occur in protein structure near position 96. It is not clear, however, why the incorporation of a new internal proton donor (Asp 46) would remove the perturbations sensed at position 96 in D96N. One possibility is that the perturbation of Asn 96 is due to the electrostatic field of a positively charged group (*e.g.*, an arginine residue (Stern & Khorana, 1989)). Such a group could form an ion pair with the carboxylate group of Asp 96 in wild-type bR and Asp 46 in the case of T46D/D96N, thereby reducing its interaction with Asn 96.

Overall, our results indicate that an Asp residue placed at position 46 can substitute for Asp 96 in the Schiff base reprotonation mechanism. This implies the following: (i) Asp 46 is located inside the Schiff base reprotonation pathway and is capable of donating a proton to the Schiff base. (ii) Similar to the native proton donor (Asp 96), Asp 46 has an anomalously high pK_a in the light-adapted form of bR. (iii) The mechanism which causes an effective drop in the pK_a of the native proton donor is still functional for Asp 46.

These results alone, however, do not establish that the Schiff base reprotonation pathway consists of a proton wire. For example, a water-filled channel might also facilitate the deprotonation of Asp 96 in wild-type bR and Asp 46 in T46D/D96N, if these residues moved from a hydrophobic to a hydrophilic environment, effectively dropping their pK_a. Future studies might resolve this ambiguity by focusing on the protonation changes of other residues which are postulated to be part of a proton wire in bacteriorhodopsin. One promising approach for this purpose would be the combination of site-directed isotope labeling and FTIR difference spectroscopy which allows band assignments to be made to individual groups in a protein (Sonar et al., 1994a; Ludlam et al., 1995).

ACKNOWLEDGMENT

We gratefully acknowledge Dr. H. G. Khorana for supplying plasmids pMPK39 and pMPK62 and MPK40 cells; Dr. J. K. Lanyi for supplying D96N bR samples; Dr. M. Krebs and Dr. R. Needleman for technical advice; and A. W. Alberts and Merck Research Laboratories for providing us with the antibiotic lovastatin used for selection of the pMPK derived plasmids. In addition, we thank S. Sonar, G. Ludlam, C. F. C. Ludlam, and J. Olejnik for critical review of the manuscript.

REFERENCES

Argade, P. V., & Rothschild, K. J. (1982) *Methods Enzymol. 88*, 643−648.
Bousché, O., Braiman, M., He, Y. W., Marti, T., Khorana, H. G., & Rothschild, K. J. (1991) *J. Biol. Chem. 266*, 11063−11067.
Bousché, O., Sonar, S., Krebs, M. P., Khorana, H. G., & Rothschild, K. J. (1992) *Photochem. Photobiol. 56*, 1085−1096.
Braiman, M. S., Mogi, T., Marti, T., Stern, L. J., Khorana, H. G., & Rothschild, K. J. (1988) *Biochemistry 27*, 8516−8520.
Braiman, M. S., Bousché, O., & Rothschild, K. J. (1991) *Proc. Natl. Acad. Sci. U.S.A. 88*, 2388−2392.
Brown, L. S., Zimanyi, L., Needleman, R., Ottolenghi, M., & Lanyi, J. K. (1993) *Biochemistry 32*, 7679−7685.
Brown, L. S., Yamazaki, Y., Maeda, A., Sun, L., Needleman, R., & Lanyi, J. K. (1994) *J. Mol. Biol. 239*, 401−414.
Butt, H. J., Fendler, K., Bamberg, E., Tittor, J., & Oesterhelt, D. (1989) *EMBO J. 8*, 1657−1663.
Cao, Y., Varo, G., Chang, M., Ni, B., Braiman, M. S., Needleman, R., & Lanyi, J. K. (1991) *Biochemistry 30*, 10972−10979.
Cao, Y., Varo, G., Klinger, A., Czajkowsky, D. M., Braiman, M. S., Needleman, R., & Lanyi, J. K. (1993) *Biochemistry 32*, 1981−1990.
Danshina, S. V., Drachev, L. A., Kaulen, A. D., Khorana, H. G., Marti, T., Mogi, T., & Skulachev, V. P. (1992) *Biokhimiya (Moscow) 57*, 1574−1585.
Drachev, L. A., Kaulen, A. D., Korana, H. G., Mogi, T., Otto, H., Skulachev, V. P., Heyn, M. P., & Holz, M. (1989) *Biokhimiya (Moscow) 54*, 1467−1477.
Duñach, M., Berkowitz, S., Marti, T., He, Y. W., Subramaniam, S., Khorana, H. G., & Rothschild, K. J. (1990a) *J. Biol. Chem. 265*, 16978−16984.
Duñach, M., Marti, T., Khorana, H. G., & Rothschild, K. J. (1990b) *Proc. Natl. Acad. Sci. U.S.A. 87*, 9873−9877.
Fodor, S. P. A., Ames, J. B., Gebhard, R., Van den Berg, E. M. M., Stoeckenius, W., Lugtenburg, J., & Mathies, R. A. (1988) *Biochemistry 27*, 7097−7101.
Gerwert, K., Hess, B., Soppa, J., & Oesterhelt, D. (1989) *Proc. Natl. Acad. Sci. U.S.A. 86*, 4943−4947.
Henderson, R., Baldwin, J. M., Ceska, T. A., Zemlin, F., Beckmann, E., & Downing, K. H. (1990) *J. Mol. Biol. 213*, 899−929.

Hessling, B., Souvignier, G., & Gerwert, K. (1993) *Biophys. J. 65*, 1929−1941.
Ho, S. N., Hunt, H. D., Horton, R. M., Pullen, J. K., & Pease, L. R. (1989) *Gene 77*, 51−69.
Kataoka, M., Kamikubo, H., Tokunga, F., Brown, L. S., Yamazaki, Y., Maeda, A., Sheves, M., Needleman, R., & Lanyi, J. K. (1994) *J. Mol. Biol. 243*, 621−638.
Krebs, M. P., Hauss, T., Heyn, M. P., RajBhandary, U. L., & Khorana, H. G. (1991) *Proc. Natl. Acad. Sci. U. S. A. 88* (3), 859−863.
Krebs, M. P., Mollaaghababa, R., & Khorana, H. G. (1993) *Proc. Natl. Acad. Sci. U.S.A. 90*, 1987−1991.
Lanyi, J. K. (1992) *J. Bioenerg. Biomembr. 24*, 169−179.
Lanyi, J. K. (1993) *Biochim. Biophys. Acta 1183*, 241−261.
Ludlam, C. F. C., Sonar, S., Lee, C.-P., Coleman, M., Herzfeld, J., RajBhandary, U. L., & Rothschild, K. J. (1995) *Biochemistry 34*, 2−6.
Maeda, A., Sasaki, J., Shichida, Y., Yoshizawa, T., Chang, M., Ni, B., Needleman, R., & Lanyi, J. K. (1992) *Biochemistry 31*, 4684−4690.
Marti, T., Otto, H., Mogi, T., Rosselet, S. J., Heyn, M. P., & Khorana, H. G. (1991) *J. Biol. Chem. 266*, 6919−6927.
Mathies, R., Freedman, T. B., & Stryer, L. (1977) *J. Mol. Biol. 109*, 367−372.
Mogi, T., Stern, L. J., Marti, T., Chao, B. H., & Khorana, H. G. (1988) *Proc. Natl. Acad. Sci. U.S.A. 85*, 4148−4152.
Nakagawa, M., Maeda, A., Ogura, T., & Kitagawa, T. (1991) *J. Mol. Struct. 242*, 221−234.
Oesterhelt, D., & Stoeckenius, W. (1974) *Methods Enzymol. 31*, 667−676.
Ormos, P. (1991) *Proc. Natl. Acad. Sci. U.S.A. 88* (2), 473−477.
Otto, H., Marti, T., Holz, M., Mogi, T., Lindau, M., Khorana, H. G., & Heyn, M. P. (1989) *Proc. Natl. Acad. Sci. U.S.A. 86*, 9228−9232.
Otto, H., Marti, T., Holz, M., Mogi, T., Stern, L. J., Engel, F., Khorana, H. G., & Heyn, M. P. (1990) *Proc. Natl. Acad. Sci. U.S.A. 87*, 1018−1022.
Pfefferlé, J. M., Maeda, A., Sasaki, J., & Yoshizawa, T. (1991) *Biochemistry 30*, 6548−6556.
Rath, P., Krebs, M. P., He, Y.-W., Khorana, H. G., & Rothschild, K. J. (1993a) *Biochemistry 32*, 2272−2281.
Rath, P., Marti, T., Sonar, S., Khorana, H. G., & Rothschild, K. J. (1993b) *J. Biol. Chem. 268*, 17742−17749.
Roepe, P., Ahl, P. L., Das Gupta, S. K., Herzfeld, J., & Rothschild, K. J. (1987) *Biochemistry 26*, 6696−6707.
Rothschild, K. J. (1992) *J. Bioenerg. Biomembr. 24*, 147−167.
Rothschild, K. J., & Sonar, S. (1995) in *CRC Handbook of Organic Photochemistry and Photobiology* (Song, P.-S., Ed.) CRC Press, London (in press).
Rothschild, K. J., Roepe, P., Lugtenburg, J., & Pardoen, J. A. (1984) *Biochemistry 23*, 6103−6109.
Rothschild, K. J., He, Y. W., Sonar, S., Marti, T., & Khorana, H. G. (1992) *J. Biol. Chem. 267*, 1615−1622.
Rothschild, K. J., Marti, T., Sonar, S., He, Y. W., Rath, P., Fischer, W., Bousche, O., & Khorana, H. (1993) *J. Biol. Chem. 268*, 27046−27052.
Sambrook, J., Fritsch, E. F., & Maniatis, T. (1989) *Molecular cloning: a laboratory manual*, 2nd ed., Cold Spring Harbor Laboratory, Cold Spring Harbor, NY.
Sasaki, J., Shichida, Y., Lanyi, J. K., & Maeda, A. (1992) *J. Biol. Chem. 267*, 20782−20786.
Sonar, S., Krebs, M. P., Khorana, H. G., & Rothschild, K. J. (1993) *Biochemistry 32*, 2263−2271.
Sonar, S., Lee, C.-P., Coleman, M., Patel, N., Liu, X., Marti, T., Khorana, H. G., RajBhandary, U. L., & Rothschild, K. J. (1994a) *Nature, Struct. Biol. 1*, 512−517.
Sonar, S., Marti, T., Rath, P., Fischer, W., Coleman, M., Nilsson, A., Khorana, H. G., & Rothschild, K. J. (1994b) *J. Biol. Chem. 269*, 28851−28858.
Steinhoff, H. J., Mollaaghababa, R., Altenbach, C., Hideg, K., Krebs, M., Khorana, H. G., & Hubbell, W. L. (1994) *Science 266*, 105−107.
Stern, L. J., & Khorana, H. G. (1989) *J. Biol. Chem. 264*, 14202−14208.
Stern, L. J., Ahl, P. L., Marti, T., Mogi, T., Duñach, M., Berkowitz, S., Rothschild, K. J., & Khorana, H. G. (1989) *Biochemistry 28*, 10035−10042.
Stoeckenius, W., & Bogomolni, R. A. (1982) *Annu. Rev. Biochem. 51*, 587−616.
Subramaniam, S., Greenhalgh, D. A., Rath, P., Rothschild, K. J., & Khorana, H. G. (1991) *Proc. Natl. Acad. Sci. U.S.A. 88*, 6873−6877.
Subramaniam, S., Gerstein, M., Oesterhelt, D., & Henderson, R. (1993) *EMBO J. 12*, 1−8.
Thorgeirsson, T. E., Milder, S. J., Miercke, L. J. W., Betlach, M. C., Shand, R. F., Stroud, R. M., & Kliger, D. S. (1991) *Biochemistry 30*, 9133−9142.
Tittor, J., Soell, C., Oesterhelt, D., Butt, H. J., & Bamberg, E. (1989) *EMBO J. 8*, 3477−3482.
Tittor, J., Schweiger, U., Oesterhelt, D., & Bamberg, E. (1994) *Biophys. J. 67*, 1682−1690.
Varo, G., & Lanyi, J. K. (1991) *Biochemistry 30*, 5008−5015.
Zhou, F., Windemuth, A., & Schulten, K. (1993) *Biochemistry 32*, 2291−2306.

BI951478W